Fundamental Research 5 (2025) 654–662

Contents lists available at ScienceDirect

Fundamental Research

journal homepage: http://www.keaipublishing.com/en/journals/fundamental-research/

Article

Pnictogen bonding enabled photosynthesis of chiral selenium-containing pyridines from pyridylphosphonium salts

Qiang Liu[a,1], Bei-Bei Zhang[a,1], Chao-Shen Zhang[a], Jia-Nan Han[a], Zhi-Xiang Wang[a,b,*], Xiang-Yu Chen[a,b,*]

[a] School of Chemical Sciences, University of the Chinese Academy of Sciences, Beijing 100049, China
[b] Binzhou Institute of Technology, Weiqiao-UCAS Science and Technology Park, Binzhou 256606, China

ARTICLE INFO

Article history:
Received 7 November 2022
Received in revised form 17 February 2023
Accepted 17 March 2023
Available online 20 April 2023

Keywords:
Pyridylphosphonium salts
Visible light-induced synthesis
Selenium-containing pyridines
Pnictogen bonding
Charge transfer complex

ABSTRACT

Pyridylphosphonium salts, which are readily available and air and thermally stable, have been used to effectively synthesize structurally diverse pyridines. Herein, we report the pnictogen bonding (PnB) enabled photoactivation of pyridylphosphonium salts with catalytic potassium carbonate to generate pyridyl radical for pyridine synthesis. Remarkably, this light-driven transformation allowed chiral pool synthesis with excellent chirality retention, giving a wide range of chiral selenium-containing pyridines. On the basis of our combined computational and experimental studies, we propose that the PnB between pyridylphosphonium salts and potassium carbonate enables access to the photoactive charge transfer complex, which is able to undergo single electron transfer to generate pyridyl radical for its transformation.

1. Introduction

Pyridine frameworks are present in a wide range of natural products, pharmaceuticals, and ligands [1–7]. Thus, a large number of novel protocols for their synthesis have been developed [8–12]. However, the asymmetric synthesis of complex chiral pyridines remains a daunting challenge. Although chiral building block [13], chiral auxiliary [14], asymmetric catalysis [15–25], and desymmetrization [26,27] strategies have been used to dictate enantioselectivity (Fig. 1a), these methods suffer some inherent limitations such as the limited availability of structurally flexible chiral pyridines, especially the structurally complex ones, and the lack of efficient methods to properly address regioselectivity and/or multistep preparation of starting pyridines.

By employing pyridylphosphonium salts, phosphorus ligand-mediated coupling developed by McNally has emerged as a viable synthetic tool for C4-pyridine functionalization (Fig. 1b, strategy i) [28–32]. However, the chiral transformations of pyridylphosphonium salts remain an open problem because the often-required stoichiometric strong base would compromise the chiral integrity. Radical-radical couplings of heterocyclic phosphonium salts have also been developed by McNally via inner-sphere electron transfer mechanism [33] or photoredox catalysts [34] (Fig. 1b, strategies ii and iii). On the other hand, the pnictogen bonding (PnB) methodology, a sigma (σ)-hole-based interaction [35] to abstract electron donor molecules, has emerged as a promising tool for the development of new concepts and reactions in organic chemistry [36–40]. Recent studies from Gabbaï [41–48], Matile [49–53], and Tan [54] have revealed the use of PnB in several ionic reactions (Fig. 1c, left). Very recently, we have demonstrated that the σ-hole bonding of phosphonium salts can be leveraged in a photoredox platform to enable a single electron transfer (SET) process (Fig. 1c, right) [55–57]. However, the σ-hole PnB of pnictogen salts is very sensitive to the steric hindrance [35–40], the large size of substituents would block the PnB formation.

Given the wide applications of pyridines, we herein explored whether it is possible to construct photoactive charge transfer complexes (CTCs) via PnB interaction between a small electron donor molecule and pyridylphosphonium salts, which deliver pyridyl radicals under visible light irradiation. The resultant pyridyl radicals then react with chiral pool materials to access chiral pyridines. We expected that mild experimental conditions would benefit chirality retention.

* Corresponding authors.
E-mail addresses: zxwang@ucas.ac.cn (Z.-X. Wang), chenxiangyu20@ucas.ac.cn (X.-Y. Chen).
[1] These authors contributed equally to this work.

https://doi.org/10.1016/j.fmre.2023.03.013

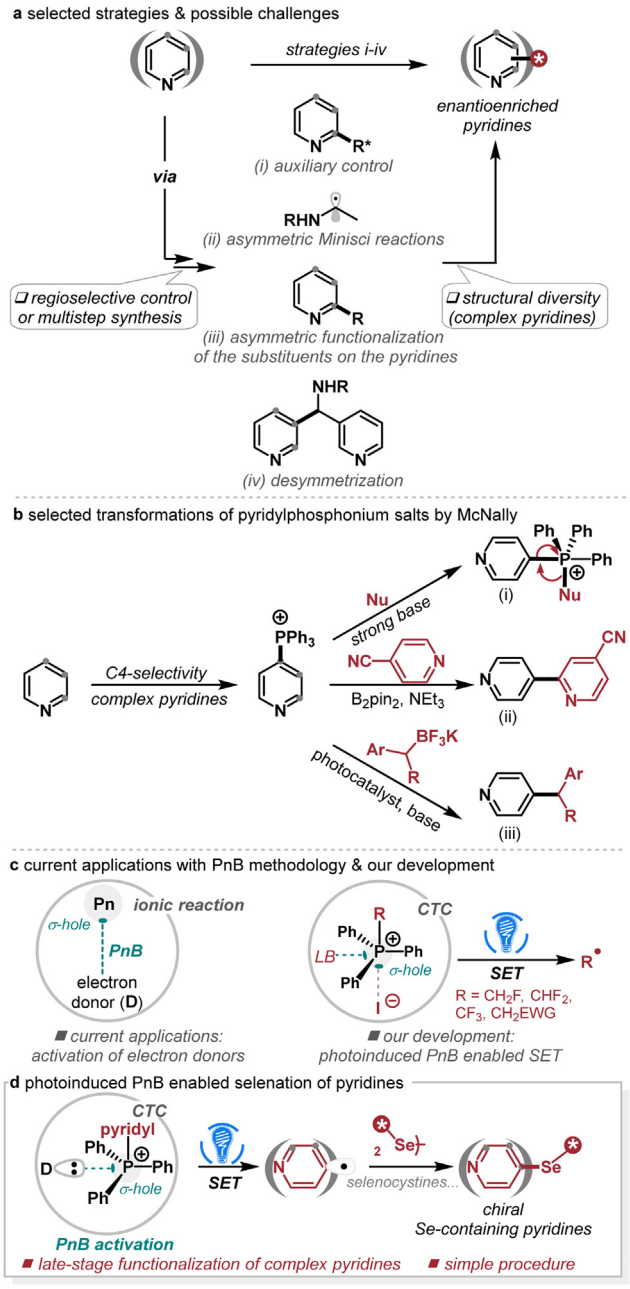

Fig. 1. (a) Selected methods for the synthesis of chiral pyridines and possible challenges; (b) selected methods for C4-pyridine functionalization via pyridylphosphonium salts; (c) current applications of PnB and our development; (d) working hypothesis of photoinduced PnB enabled SET for the synthesis of chiral Se-containing pyridines.

In the meantime, selenium (Se)-containing compounds, which are commonly used as catalysts, ligands, semiconductors, and photovoltaic materials, have always been an inspiration for chemists to design a number of strategies for their synthesis [58–66]. In particular, the chiral ones (e.g., selenocysteine, the 21st amino acid) have remarkable biological properties, such as protection against oxidative stress in various organisms; activation of thyroid hormones through deiodinations; reducing age-related disorders and antiviral properties [67]. We, therefore, set out to devise a method for accessing diverse chiral Se-containing pyridines, including asymmetric late-stage structural modification of complex pyridines, via the PnB-directed SET process with readily available pyridylphosphonium salts (Fig. 1d).

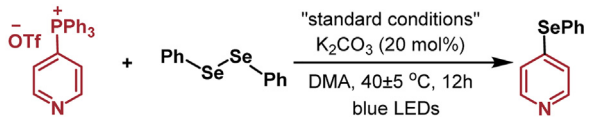

Entry	Variations from standard conditions	Yield [%][a]
1	none	97
2	without K_2CO_3	49
3	$KHCO_3$ instead of K_2CO_3	78
4	NaOAc instead of K_2CO_3	87
5	Na_2CO_3 instead of K_2CO_3	80
6	KH_2PO_4 instead of K_2CO_3	35
7	Cs_2CO_3 instead of K_2CO_3	92
8	other solvents (e.g. CH_3CN, DCM, DMF...)	trace-70
9	without visible-light irradiation	NR
10	addition of TEMPO (3.0 equiv.)	NR

Fig. 2. Optimization of the reaction conditions. Yield of isolated product **3** after chromatography.

2. Materials and methods/experiment

2.1. General procedure for the synthesis of pyridyl selenides/sulfides

In a nitrogen-filled glove box, a 10-mL vial equipped with a magnetic stirring bar was charged sequentially with diselenide/disulfide (0.15 mmol, 1.0 equiv.), triphenylphosphonium salt (0.30 mmol, 2.0 equiv.), K_2CO_3 (20 mol%) and DMA/DMF (1.5 mL). The vial was closed and removed from the glove box. The resulting mixture was stirred under blue LED (40 W) irradiation for overnight as monitored by TLC. The reaction temperature was monitored by the IR Thermometer (TA601B), which showed the temperature was 40 ± 5 °C. Upon completion, solvent was removed under vacuum and the residue was subjected to silica gel chromatography using petroleum ether and ethyl acetate as eluent to afford the desired product.

2.2. General procedure for the synthesis of chiral pyridyl selenides

In a nitrogen-filled glove box, a 10-mL vial equipped with a magnetic stirring bar was charged sequentially with chiral diselenide (0.10 mmol, 1.0 equiv.), triphenylphosphonium salt (0.20 mmol, 2.0 equiv.), K_2CO_3 (20 mol%) and DCM (1.0 mL). The vial was closed and removed from the glove box. The resulting mixture was stirred under blue LED (100 W) irradiation for overnight as monitored by TLC. The reaction temperature was monitored by the IR Thermometer (TA601B), which showed the temperature was 45 ± 5 °C. Upon completion, solvent was removed under vacuum and the residue was subjected to silica gel chromatography using petroleum ether and ethyl acetate as eluent to afford the desired product.

3. Results and discussion

3.1. Reaction optimization

Toward our goal, we began our research by investigating the selenation of pyridylphosphonium salts (Fig. 2). Our exploration of the process led us identify a simple reaction condition. The reaction using pyridylphosphonium salt **1** and diphenyl diselenide **2** as the substrates, 20 mol% of K_2CO_3 as the base, DMA as the solvent, under blue light irradiation, afforded the desired product **3** in 97% yield (entry 1). The reactivity was significantly decreased in the absence of K_2CO_3, giving 49% yield (entry 2). Other bases, such as Na_2CO_3, Cs_2CO_3, $KHCO_3$, NaOAc, and KH_2PO_4 delivered inferior results (entries 3–7). The screening of the influence of solvents showed that DMA was the best choice

(entry 8). The reaction did not proceed without light, suggesting the essential role of light (entry 9). Furthermore, complete inhibition of the reaction was observed by the addition of TEMPO to the standard reaction conditions, indicating the reaction might undergo a radical pathway (entry 10).

3.2. Substrate scope

With the optimized reaction conditions in hand, the reaction scope was briefly investigated (Fig. 3). Both electron-donating (3-Me, 3-OMe and 3-Ph) and electron-withdrawing (3-Br, 3-CN and 3-CO_2Me) groups on the pyridyl ring of pyridylphosphonium salts were tolerable and afforded the desired products **3–9** in moderate to high yields. The *ortho*-substituent (2-Ph) was also tolerated (**10**). That was also true for the disubstituted substrate (**11**). In addition, substrates bearing electron-withdrawing (Cl, CN and CF_3) and electron-donating groups (Me and OMe) at the *para*-, *meta*-, or *ortho*-position of the benzene ring of diselenides, furnished the corresponding products **12–17** in 51%–87% yields. Notably, the dimethyl diselenide was also successful and provided the desired product **18** in 58% yield. Furthermore, we successfully achieved selective functionalization of several drug-like fragments by using the developed strategy. Pyridine-containing compounds, appended with other nitrogen heterocycles including piperazine, oxazole, piperidine, pyrimidine, and quinoline are all effective (**19–24**). Gratifyingly, Loratadine, Abiraterone acetate, Bisacodyl, Etoricoxib, and Pyriproxyfen could readily undergo selenation and afforded the desired compounds with good reaction efficiency (**25–29**). To expand the synthetic utility of this strategy, a convenient protocol for the synthesis of the pyridyl sulfides was also achieved. It was demonstrated that pyridylphosphonium salts possessing substituents, such as Ph, OMe, Me, Br, CN, and CO_2Me, at the C2 and C3 positions all worked well, providing the corresponding products **30–37** in 50%–98% yields. The disubstituted substrate was also tolerant to deliver the desired product **38** in 71% yield. The diaryl sulfides with electron-donating (4-Me, 4-MeO and 2-PhCONH) or withdrawing (4-Cl, 4-Br, 4-CN, 3-F and 3,5-di-Cl) groups on the phenyl group led to the targeted compounds **39–46** in moderate to good yields. Heterocyclic disulfides such as thienyl disulfide, pyridyl disulfide, and furyl disulfide were also effective with this strategy (**47–49**). Furthermore, the late-stage functionalization of drug-like fragments and pharmaceutical compounds was also successfully obtained with satisfactory outcomes (**50–58**). Note that phenylsulfanylsulfonylbenzene was also tolerant to afford the desired product **30** in 75% yield. Nevertheless, attempts to synthesize pyridyl tellurides with diphenyl ditelluride gave the desired product in very low yield (<10%, see SI for detailed results).

Chiral transformations of pyridylphosphonium salts have not been achieved, probably due to the necessity of strong base that compromises the chiral integrity. Given our mild experimental conditions using catalytic weak base (20 mol %K_2CO_3), we further examined the developed strategy to prepare chiral Se-containing pyridines via chiral pool synthesis (Fig. 4). To our delight, all the transformations described below have excellent chirality retention. Selenocysteines bearing different chiralities (*L*- and *D*−selenocysteines) showed efficient reactivity with pyridylphosphonium salt **1** and resulted in products **59** and **60** in moderate yields with excellent chirality retention. The synthetic utility of the present strategy was further evaluated for the synthesis of various chiral *β*-seleno amines [68,69]. A series of chiral diselenides derived from alaninols, valines, leucenols, and phenylalanyls all reacted smoothly to give the desired chiral pyridines bearing *β*-seleno amines **61–70** in 48%–58% yields with uniformly high ee. That was also true for the chiral pyridinemethanol-derived substrates (**71** and **72**). The glycerol derivatives containing seleniums have shown promising pharmacology properties, such as inhibition of linoleic acid lipid peroxidation [60]. As shown in Fig. 4, the reactions of glycerol-derived diselenides led to the desired products **73** and **74** in 49% and 53% yields with > 99% ee, respectively. Notably, sugar derivatives also worked well in the reaction (**75** and **76**).

Given the wide biological functions of selenocysteines, we next turn our attention to the synthesis of various chiral selenocysteine-containing pyridines. The electronic nature of the substituents on pyridines had no significant effect on the reactivity, neither electron-withdrawing nor electron-donating groups. For example, the 2-Ph, 2-Me, 2-CO_2Me, 3-OMe, 3-Me, 3-F, 3-Cl, and 3-CO_2Me substituted pyridylphosphonium salts all worked well and gave the desired products with excellent ee (**77–90**). The disubstituted substrates worked as well (**91** and **92**). Pyridines derived from diverse scaffolds were all converted into the corresponding products **93–108** in 43%–76% yields with > 99% ee under the reaction conditions. Note that the phosphorus ligand-mediated coupling strategy [31,32] fails to produce chiral selenocysteine-containing pyridine in the presence of a strong base (Formula 1).

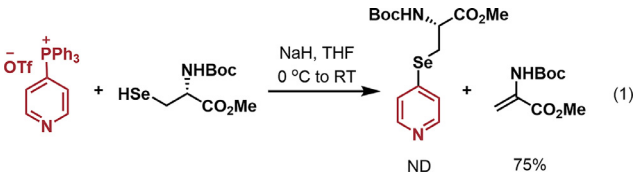

3.3. Mechanistic discussion

To understand the reaction mechanism, a series of mechanistic experiments were conducted (Fig. 5). A possible pathway via direct photolysis of the pyridylphosphonium salt could be safely ruled out, because the photolysis experiment recovered the salt **1** in 92% yield (Fig. 5a). Interestingly, when adding K_2CO_3 to the solution of salt **1**, the reaction gave pyridyl radical dimerization product **109**. Furthermore, the yield of **109** increased as the concentration of K_2CO_3 increased and no **109** could be observed in the absence of light irradiation (Fig. 5b). These experiments indicated that the transformation could involve pyridyl radical and that K_2CO_3 played an important role for the photoactivation of **1** to generate the radical presumably via forming a photoactive complex with the salt. To understand the role of K_2CO_3, we performed UV–vis spectrum study. As compared in Fig. 5c, while the salt **1** and K_2CO_3 alone showed negligible absorption in the visible light region, the spectrum of their mixture tailed to the visible light region significantly. Similarly, the mixture of **1** and dimethyl diselenide also showed enhanced absorption compared to dimethyl diselenide. On the basis of these experimental studies, along with the fact that the addition of K_2CO_3 to the reaction of pyridylphosphonium salt **1** with diphenyl diselenide **2** nearly doubled the yield of the product **3** (Fig. 2, entries 1 and 2), we proposed two possible pathways which involve a photoactive charge transfer complex (CTC) formed between pyridylphosphonium salt **1** and diselenide (pathway 1, Fig. 5d, left) or between pyridylphosphonium salt **1** and K_2CO_3 (pathway 2, Fig. 5d, right) with pathway 2 being more effective.

In our proposed pathways, the pyridyl radical from photoactivation of the CTC complex participates in subsequent reaction steps. Previously, it was postulated that the photoactivation of pyridylphosphonium salts results in phosphonium radical anion for subsequent reaction steps without breaking the C-P bond [33,34]. To explore the possibility, we performed the reaction using allyloxy substituted pyridylphosphonium salt (Fig. 5e), with the expectation that the bulky PPh_3 group would prevent the radical anion from undergoing cyclization. However, we observed the cyclization product by GCMS. Thus, it is unlikely that the reaction uses phosphonium radical anion for subsequent reaction steps. As will be discussed further, our DFT calculations show this is indeed the case (vide infra). Attempts were made to trap the pyridyl radical with TEMPO, DMPO, DPPH, PBN, and *m*-xyloquinone. Although we were not able to characterize the pyridyl radical trapping adducts, the reaction was completely inhibited (see SI for details).

According to our proposed mechanism, the reaction led to selenophosphonium salt as the byproduct, seemingly contradicting to the us-

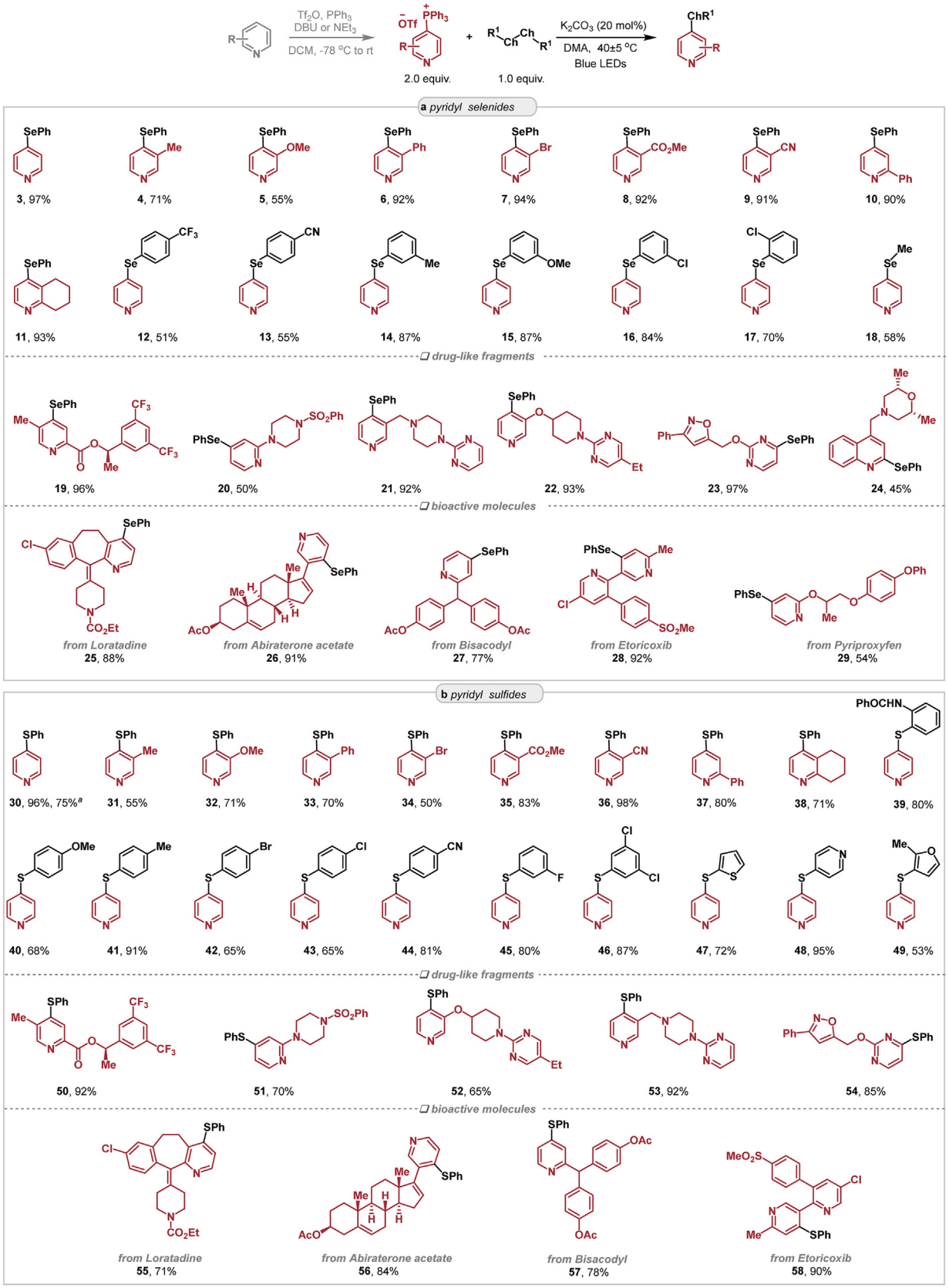

Fig. 3. Scope of photoinduced PnB strategy for the coupling of pyridylphosphonium salts with dichalcogenides. Yield of isolated product given. (a) Preparation of pyridyl selenides; (b) preparation of pyridyl sulfides, DMF was used as the solvent instead of DMA. [a] Phenylsulfanylsulfonylbenzene was used instead of phenyl disulfide.

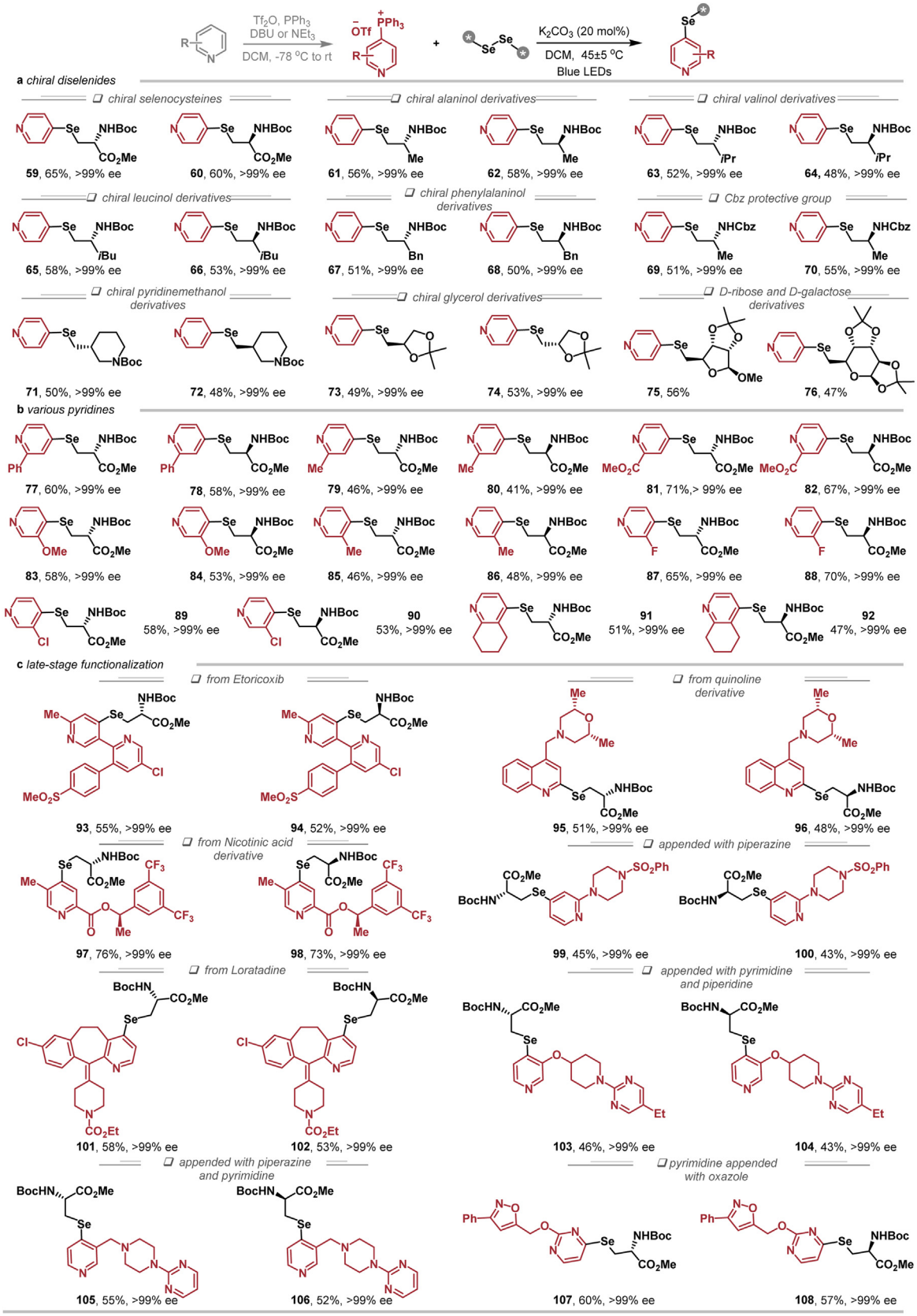

Fig. 4. Applications of photoinduced PnB strategy for the synthesis of chiral pyridines. Yield of isolated product given; ee value was determined by HPLC analysis of the purified product on a chiral stationary phase.

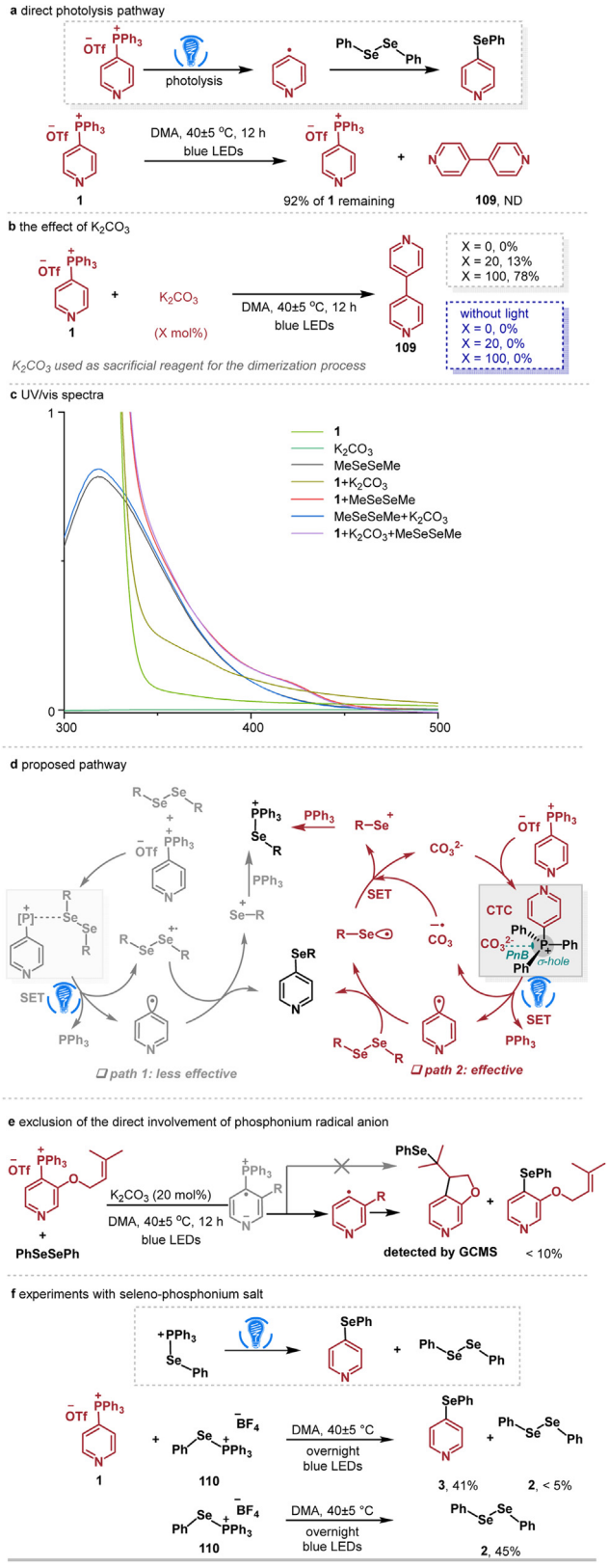

Fig. 5. Mechanistic investigations. (a) Photolysis experiment; (b) the effect of K_2CO_3 in the photoactivation of pyridylphosphonium salts; (c) UV/vis spectra of **1** (10^{-2} M), K_2CO_3 (2×10^{-3} M), MeSeSeMe (10^{-2} M) and the corresponding mixtures in DMA; (d) proposed pathways; (e) exclusion of the direct involvement of phosphonium radical anion; (f) experiments with seleno-phosphonium salt.

age of 2:1 ratio of the salt and diselenide. We envisioned that the byproduct seleno-phosphonium salt must further react with the pyridylphosphonium salt to give the desired product. To demonstrate this, we subjected seleno-phosphonium salt **110** to **1** and obtained product **3** in 41% yield. In addition, the irradiation of seleno-phosphonium salt led to the diselenide **2** in 45% yield (Fig. 5f). Therefore, the seleno-phosphonium salt could be recycled to the corresponding diselenide for further reaction, reconciling the seeming contradiction.

To elaborate the reaction pathways and support our mechanistic proposal, density functional theory (DFT) and time-dependent DFT (TDDFT) calculations were performed (see SI for computational details), using the reaction of pyridylphosphonium salt **1** and dimethyl diselenide **DSe** (Fig. 6). In terms of binding free energy and photoactivity, we examined several possibilities for the complexations of **1**, **DSe**, and K_2CO_3 and obtained an optimal structure ^{1}**CT1** that we considered to be the photoactive CTC (see SI for alternatives). Supportively, ^{1}**CT1** was predicted to feature a maximum absorption wavelength (420 nm) in the visible light region and the formation of ^{1}**CT1** is energetically favorable. Subsequently, ^{1}**CT1** is excited to ^{1}**CT1*** in the first singlet excited state (S1 state) under blue light irradiation, followed by structural relaxation to an equilibrium structure ^{1}**CT1eq*** in S1 state. Examining the frontier orbitals of ^{1}**CT1** shows that the excitation results in a SET from the lone pair orbital of K_2CO_3 to the antibonding π orbital of **1** cation, mainly located on the pyridyl moiety. Afterwards, three possible mechanisms could operate to liberate pyridyl radical (denoted as ^{2}**IM2**) from ^{1}**CT1eq***: (path a) ^{1}**CT1eq*** first releases $K_2CO_3^{\bullet+}$ to give $PPh_3Py^\bullet$ (^{2}**IM1**) which then undergoes C-P bond cleavage via ^{2}**TS2** to afford ^{2}**IM2**. Relative to ^{1}**CT1eq***, the process overcomes a barrier of 16.7 kcal mol^{-1} and is endergonic by 11.2 kcal mol^{-1}. (path b) ^{1}**CT1eq*** first undergoes intersystem crossing (ISC) to give the triplet ^{3}**CT1** which then breaks the C-P bond via ^{3}**TS1** to generate the pyridyl radical. The process is endergonic by 13.9 kcal mol^{-1} with a barrier of 21.2 kcal mol^{-1} (^{3}**TS1** relative to ^{3}**CT1**). Similar to ^{1}**CT1eq***, ^{3}**CT1** can also first release $K_2CO_3^{\bullet+}$ and finally give pyridyl radical by passing through ^{2}**IM1** and ^{2}**TS2**. (path c) It is also possible ^{1}**CT1eq*** proceeds directly along the potential energy surface of S1 state to homolytically cleave the C-P bond via a transition state, namely ^{1}**TS1***. Although we could not locate the assumed transition state due to the challenge of geometric optimizations in the excited state, the generation of pyridyl radical is easy because of the feasible pathways (a) and (b). Subsequent to the generation of the pyridyl radical ^{2}**IM2**, the radical attacks **DSe** via ^{2}**TS3** to form the C-Se bond with a barrier of 20.5 kcal mol^{-1} (^{2}**TS3** relative to ^{3}**CT1**), leading to the product **18** and meanwhile releasing MeSe$^\bullet$ radical. Finally, MeSe$^\bullet$, PPh_3, and $K_2CO_3^{\bullet+}$ undergo intermolecular SET to regenerate the catalyst K_2CO_3, giving the byproduct $MeSePPh_3^+$ which can be converted to diselenide and PPh_3 (see Fig. 5f). Overall, the reaction has accessible kinetic barriers with gradually downhill thermodynamics, rationalizing the occurrence of the reaction, which supports our proposed mechanism.

To support our speculation that a phosphonium radical anion could not directly participate in the subsequent reaction steps, we also studied the pathway of **DSe** directly attacking $PPh_3Py^\bullet$ (i.e. phosphonium radical anion, see path d in Fig. 6). As **DSe** approaches $PPh_3Py^\bullet$, a SET from the latter to the former first occurs via a transition state ^{2}**TS4**, giving an intermediate ^{2}**IM3** which can be considered as a complex between **DSe**$^{\bullet-}$ and **1** cation. This process is endergonic by 2.9 kcal mol^{-1} with a low barrier of 7.3 kcal mol^{-1}, suggesting that the SET is reversible. In **DSe**$^{\bullet-}$, the Se-Se bond is weakened. Subsequently, the C-Se bond formation and the C-P bond cleavage take place by a concerted process with a barrier of 25.7 kcal mol^{-1} (^{2}**TS5** relative to ^{2}**IM3**). Compared with the mechanism via pyridyl radical, this concerted pathway requires overcoming a higher energy barrier (^{2}**TS5**, which is more than 11.0 kcal mol^{-1} higher than ^{3}**TS1** or ^{2}**TS3**). Therefore, the phosphonium radical anion should be fragmented first to the pyridyl radical before it participates in the subsequent reaction steps.

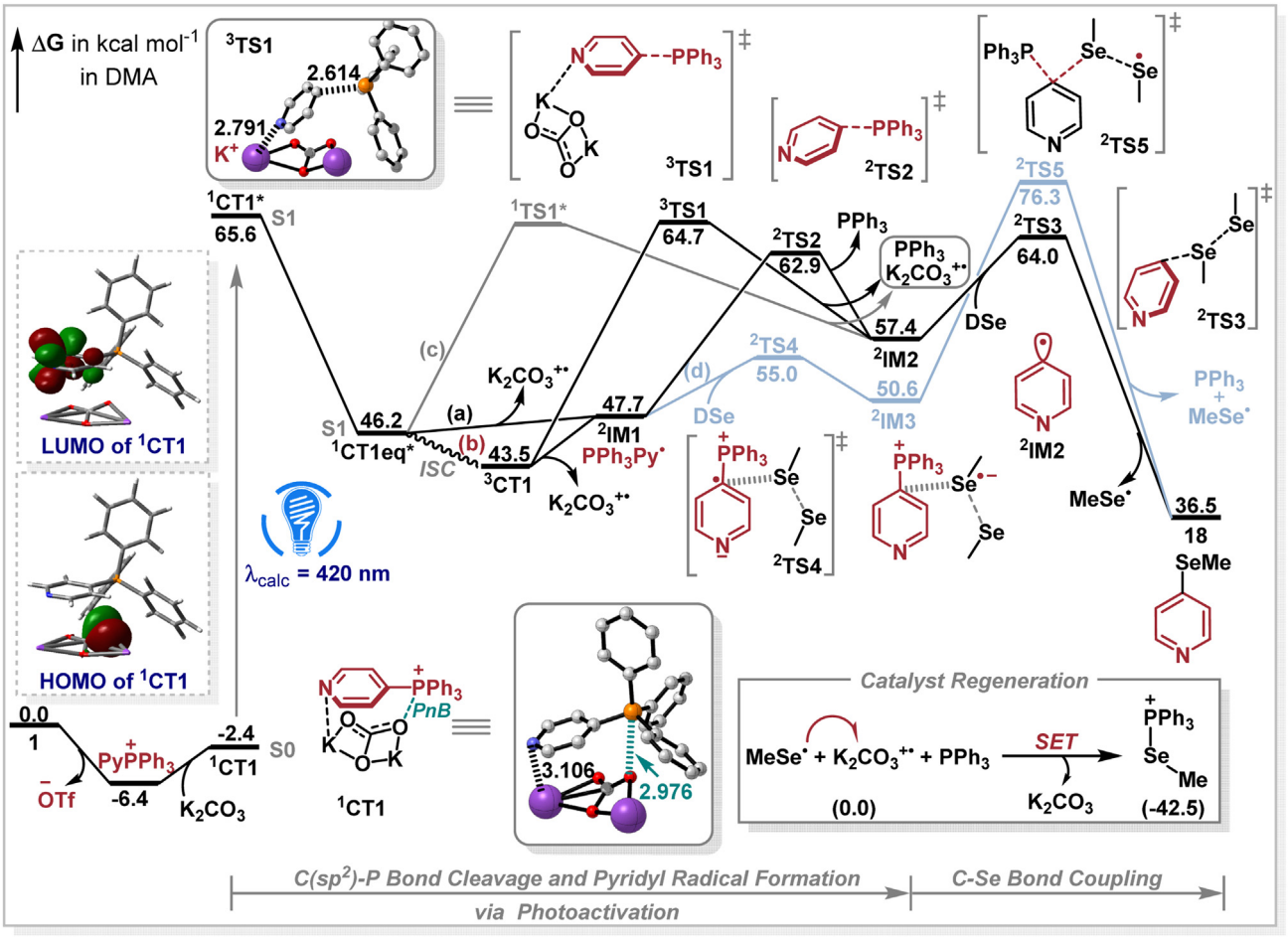

Fig. 6. Free energy profiles (in kcal mol^{-1}) for the reaction of the salt 1 with dimethyl diselenide DSe.

According to the discussion above, the photoactivation of the salt takes place at ^{1}**CT1** via SET, we thus further characterized the interaction between pyridylphosphonium salt **1** and K_2CO_3. The electrostatic potential surface (EPS) of **1** cation exhibits the σ-hole (Fig. 7a). The O···P distance (2.976 Å) is much shorter than the sum (3.320 Å) of the van der Waals radii of the two atoms [70]. The C^2-P bond is elongated by 0.018 Å, compared to that in the isolated **1** cation and the C^2-P-O angle (168°) is close to 180°. These results are consistent with the occurrence of σ-hole interaction (Fig. 7b) [36–57]. Consistently, the following noncovalent interaction (NCI) analysis [71,72] characterized the noncovalent nature of the attractive interaction in ^{1}**CT1** (green surface, Fig. 7c). Natural bond orbital (NBO) analysis [73,74] identified a weak donor-acceptor interaction between the lone pair of O and the C^1-P σ-antibonding orbital with the second-order stabilization energy of 1.42 kcal mol^{-1} (Fig. 7d). Furthermore, we performed QTAIM analysis (the quantum theory of atoms in molecules) to characterize the interaction (Fig. 7e) [75]. The approach characterizes a chemical interaction by a bond critical point (BCP) along with the values of electron density (ρ), Laplacian ($\nabla^2\rho$), and energy density (H) at BCP. A donor-acceptor interaction is typified by a small electron density and positive values of energy density and Laplacian. We were able to locate a BCP between O and P in ^{1}**CT1**. The BCP features an electron density (ρ = 0.0145 a.u.) and a positive Laplacian ($\nabla^2\rho$ = +0.0402 a.u.) and H (+0.0003 a.u.). These QTAIM results indicate the electrostatic interaction dominated weak interaction of the complex, in agreement with the occurrence of σ-hole interaction.

To verify the role of the σ-hole, we carried out the control experiments in Fig. 8. Considering the effectiveness of PnB could be affected by the directionality and steric hindrance, we prepared the

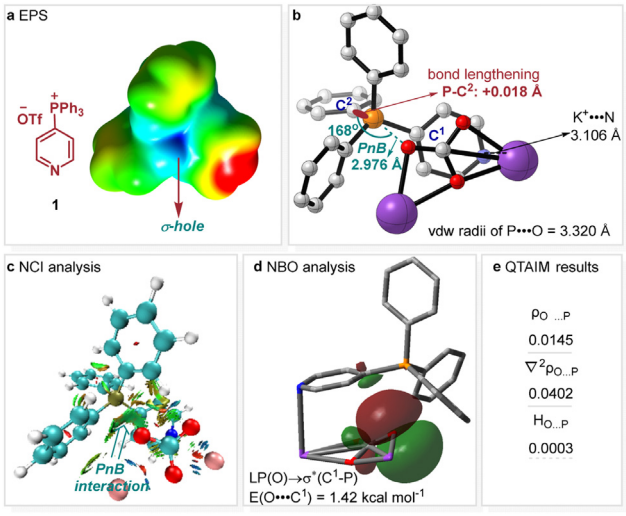

Fig. 7. (a) EPS of pyridylphosphonium salt (isosurface: 0.0004 a.u., red: 0.05 a.u., blue: 0.143 a.u.); (b) optimized structure of ^{1}**CT1**, with bond lengths and angles; (c) NCI plot isosurfaces in the complex of ^{1}**CT1**; (d) NBO analysis of ^{1}**CT1**; (e) results of quantum theory of atoms in molecules (QTAIM) analysis showing O···P noncovalent interaction.

para- (4-Me and 4-OMe) and *ortho*-substituted (2-Me and 2,6-di-OMe) pyridylphosphonium salts and compared their performances under the optimal conditions. Comparing Fig. 8a and 8b, the *para*-substituted

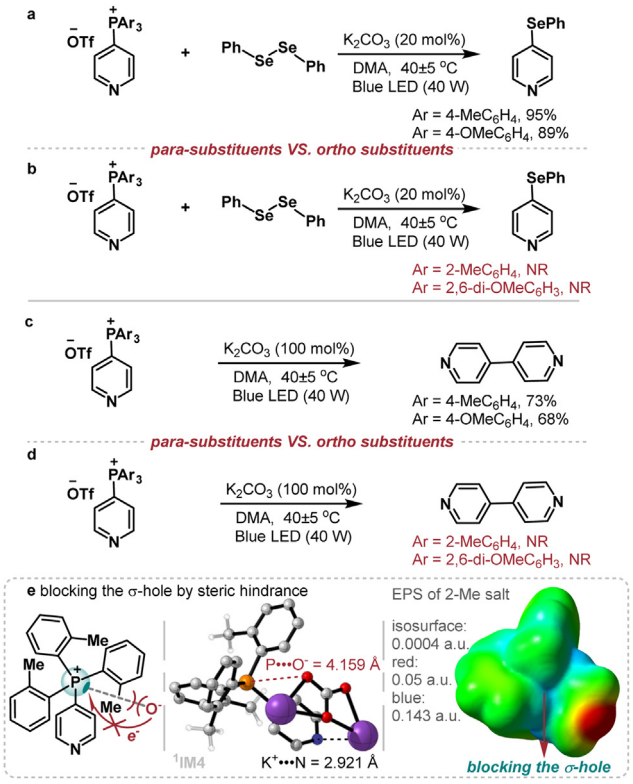

Fig. 8. Control experiments verifying the role of the σ-hole.

pyridylphosphonium salts gave the product with yields comparable to that of salt **1**, while the *ortho*-substituted salts afforded no desired product. The same holds true for the dimerization experiments, comparing Fig. 8c and 8d. We attributed the contrasting performance to that the *ortho*-substitutions led to severe steric hindrance that prevented the function of σ-hole (Fig. 8e). Indeed, the DFT optimized ^{1}**CT1**-like complex between 2-Me salt and K_2CO_3 has a P···O distance (4.159 Å) much longer than the 2.976 Å in ^{1}**CT1**. These results clearly demonstrate the important role of the σ-hole in this photoinduced process.

4. Conclusion

In conclusion, the photoinduced PnB-enabled functionalization of pyridylphosphonium salts with a catalytic potassium carbonate has been developed, which allowed the synthesis of various Se-containing pyridines in moderate to good yields. The methodology is characterized by operational simplicity, avoidance of transition metals, photocatalysts, and stoichiometric strong bases, and asymmetric late-stage structural modification of drug-like fragments and pharmaceutically relevant pyridine derivatives. Experimental and computational studies have indicated that the PnB of pyridylphosphonium salts facilitates the formation of a photoactive CTC with a carbonate electron donor, and the σ-hole is crucial for triggering the reaction. In light of the appealing properties of functionalized pyridines as well as the new application of PnB, it is expected to provide a new platform for the transformations of pyridylphosphonium salts. This work also constitutes a new example of how to use PnB to develop photoinduced transformations, which is pursued in our laboratory.

Declaration of competing interest

The authors declare that they have no conflicts of interest in this work.

Acknowledgments

This work was supported by grants from the National Natural Science Foundation of China (22101279, 22001248) and Fundamental Research Funds for the Central Universities, the University of the Chinese Academy of Sciences and Binzhou Institute of Technology, Weiqiao-UCAS Science and Technology Park.

Supplementary materials

Supplementary material associated with this article can be found, in the online version, at doi:10.1016/j.fmre.2023.03.013.

References

[1] G. Yang, W. Zhang, Renaissance of pyridine-oxazolines as chiral ligands for asymmetric catalysis, Chem. Soc. Rev. 47 (2018) 1783–1810.
[2] A.Y. Guan, C.L. Liu, X.F. Sun, et al., Discovery of pyridine-based agrochemicals by using Intermediate Derivatization Methods, Bioorg. Med. Chem. 24 (2016) 342–353.
[3] A.A. Altaf, A. Shahzad, Z. Gul, et al., Review on the Medicinal Importance of Pyridine Derivatives, J. Drug Des. Med. Chem. 1 (2015) 1–11.
[4] H.L. Kwong, H.L. Yeung, C.T. Yeung, et al., Chiral pyridine-containing ligands in asymmetric catalysis, Coord. Chem. Rev. 251 (2007) 2188–2222.
[5] R.P. Wurz, Chiral dialkylaminopyridine catalysts in asymmetric synthesis, Chem. Rev. 107 (2007) 5570–5595.
[6] G. Desimoni, G. Faita, P. Quadrelli, Pyridine-2,6-bis(oxazolines), helpful ligands for asymmetric catalysts, Chem. Rev. 103 (2003) 3119–3154.
[7] E. Vitaku, D.T. Smith, J.T. Njardarson, Analysis of the structural diversity, substitution patterns, and frequency of nitrogen heterocycles among U.S. FDA approved pharmaceuticals, J. Med. Chem. 57 (2014) 10257–10274.
[8] R.S.J. Proctor, R.J. Phipps, Recent advances in minisci-type reactions, Angew. Chem. Int. Ed. 58 (2019) 13666–13699.
[9] K. Murakami, S. Yamada, T. Kaneda, et al., C–H functionalization of azines, Chem. Rev. 117 (2017) 9302–9332.
[10] C. Allais, J.M. Grassot, J. Rodriguez, et al., Metal-free multicomponent syntheses of pyridines, Chem. Rev. 114 (2014) 10829–10868.
[11] V.C. Gibson, C. Redshaw, G.A. Solan, Bis(imino)pyridines: Surprisingly reactive ligands and a gateway to new families of catalysts, Chem. Rev. 107 (2007) 1745–1776.
[12] J.A. Varela, C. Saá, Construction of pyridine rings by metal-mediated [2 + 2 + 2] cycloaddition, Chem. Rev. 103 (2003) 3787–3802.
[13] C. Tanyeli, İ.M. Akhmedov, M. Işık, Synthesis of various camphor-based chiral pyridine derivatives, Tetrahedron Lett. 45 (2004) 5799–5801.
[14] S.D. Kuduk, R.M. DiPardo, R.K. Chang, et al., Reversal of diastereoselection in the addition of Grignard reagents to chiral 2-pyridyl tert-butyl (Ellman) sulfinimines, Tetrahedron Lett. 45 (2004) 6641–6643.
[15] K. Li, L. Wei, M. Sun, et al., Enantioselective synthesis of pyridines with all-carbon quaternary carbon centers via cobalt-catalyzed desymmetric [2+2+2] cycloaddition, Angew. Chem. Int. Ed. 60 (2021) 20204–20209.
[16] R.S.J. Proctor, P. Chuentragool, A.C. Colgan, et al., Hydrogen atom transfer–driven enantioselective minisci reaction of amides, J. Am. Chem. Soc. 143 (2021) 4928–4934.
[17] K. Cao, S.M. Tan, R. Lee, et al., Catalytic enantioselective addition of prochiral radicals to vinylpyridines, J. Am. Chem. Soc. 141 (2019) 5437–5443.
[18] J.J. Gladfelder, S. Ghosh, M. Podunavac, et al., Enantioselective alkylation of 2-alkylpyridines controlled by organolithium aggregation, J. Am. Chem. Soc. 141 (2019) 15024–15028.
[19] W.B. Zhang, X.T. Yang, J.B. Ma, et al., Regio- and enantioselective C–H cyclization of pyridines with alkenes enabled by a nickel/N-heterocyclic carbene catalysis, J. Am. Chem. Soc. 141 (2019) 5628–5634.
[20] A. Kundu, M. Inoue, H. Nagae, et al., Direct ortho-C-H aminoalkylation of 2-substituted pyridine derivatives catalyzed by yttrium complexes with N, N'-diarylethylenediamido ligands, J. Am. Chem. Soc. 140 (2018) 7332–7342.
[21] R.S.J. Proctor, H.J. Davis, R.J. Phipps, Catalytic enantioselective Minisci-type addition to heteroarenes, Science 360 (2018) 419–422.
[22] Y. Yin, Y. Dai, H. Jia, et al., Conjugate addition–enantioselective protonation of N-aryl glycines to α-branched 2-vinylazaarenes via cooperative photoredox and asymmetric catalysis, J. Am. Chem. Soc. 140 (2018) 6083–6087.
[23] R.P. Jumde, F. Lanza, T. Pellegrini, et al., Highly enantioselective catalytic synthesis of chiral pyridines, Nat. Commun. 8 (2017) 2058.
[24] S. Wang, X. Li, H. Liu, et al., Organocatalytic enantioselective direct additions of aldehydes to 4-vinylpyridines and electron-deficient vinylarenes and their synthetic applications, J. Am. Chem. Soc. 137 (2015) 2303–2310.
[25] G. Song, W.W.N. O, Z. Hou, Enantioselective C–H bond addition of pyridines to alkenes catalyzed by chiral half-sandwich rare-earth complexes, J. Am. Chem. Soc. 136 (2014) 12209–12212.
[26] Y. Tang, S.J. Miller, Catalytic enantioselective synthesis of pyridyl sulfoximines, J. Am. Chem. Soc. 143 (2021) 9230–9235.
[27] S.Y. Hsieh, Y. Tang, S. Crotti, et al., Catalytic enantioselective pyridine N-oxidation, J. Am. Chem. Soc. 141 (2019) 18624–18629.
[28] X. Zhang, K.G. Nottingham, C. Patel, et al., Phosphorus-mediated sp^2-sp^3 couplings for C-H fluoroalkylation of azines, Nature 594 (2021) 217–222.

[29] M.C. Hilton, X. Zhang, B.T. Boyle, et al., Heterobiaryl synthesis by contractive C-C coupling via P(V) intermediates, Science 362 (2018) 799–804.
[30] M.C. Hilton, R.D. Dolewski, A. McNally, Selective functionalization of pyridines via heterocyclic phosphonium salts, J. Am. Chem. Soc. 138 (2016) 13806–13809.
[31] R.G. Anderson, B.M. Jett, A. McNally, A unified approach to couple aromatic heteronucleophiles to azines and pharmaceuticals, Angew. Chem. Int. Ed. 57 (2018) 12514–12518.
[32] R.G. Anderson, B.M. Jett, A. McNally, Selective formation of heteroaryl thioethers via a phosphonium ion coupling reaction, Tetrahedron 74 (2018) 3129–3136.
[33] J.L. Koniarczyk, J.W. Greenwood, J.V. Alegre-Requena, et al., A pyridine–pyridine cross-coupling reaction via dearomatized radical intermediates, Angew. Chem. Int. Ed. 58 (2019) 14882–14886.
[34] J.W. Greenwood, B.T. Boyle, A. McNally, Pyridylphosphonium salts as alternatives to cyanopyridines in radical–radical coupling reactions, Chem. Sci. 12 (2021) 10538–10543.
[35] B. Mallada, A. Gallardo, M. Lamanec, et al., Real-space imaging of anisotropic charge of σ-hole by means of Kelvin probe force microscopy, Science 374 (2021) 863–867.
[36] M. Breugst, J.J. Koenig, σ-Hole Interactions in Catalysis, Eur. J. Org. Chem. 2020 (2020) 5473–5487.
[37] K.T. Mahmudov, A.V. Gurbanov, V.A. Aliyeva, et al., Pnictogen bonding in coordination chemistry, Coordin. Chem. Rev. 418 (2020) 213381.
[38] L. Vogel, P. Wonner, S.M. Huber, Chalcogen bonding: An overview, Angew. Chem. Int. Ed. 58 (2019) 1880–1891.
[39] S. Scheiner, The pnicogen bond: Its relation to hydrogen, halogen, and other noncovalent bonds, Acc. Chem. Res. 46 (2013) 280–288.
[40] R. Papagna, L. Vogel, S.M. Huber, in: Anion-Binding Catalysis, Wiley-VCH, Weinheim, 2022, pp. 307–343. (Eds.: O.G. Mancheño).
[41] V.M. Gonzalez, G. Park, M. Yang, et al., Fluoride anion complexation and transport using a stibonium cation stabilized by an intramolecular P=O → Sb pnictogen bond, Dalton Trans. 50 (2021) 17897–17900.
[42] G. Park, F.P. Gabbaï, Redox-controlled chalcogen and pnictogen bonding: The case of a sulfonium/stibonium dication as a preanionophore for chloride anion transport, Chem. Sci. 11 (2020) 10107–10112.
[43] G. Park, D.J. Brock, J.P. Pellois, et al., Heavy pnictogenium cations as transmembrane anion transporters in vesicles and erythrocytes, Chem 5 (2019) 2215–2227.
[44] M. Yang, M. Hirai, F.P. Gabbaï, Phosphonium–stibonium and bis-stibonium cations as pnictogen-bonding catalysts for the transfer hydrogenation of quinolines, Dalton Trans. 48 (2019) 6685–6689.
[45] M. Yang, N. Pati, G. Bélanger-Chabot, et al., Influence of the catalyst structure in the cycloaddition of isocyanates to oxiranes promoted by tetraarylstibonium cations, Dalton Trans. 47 (2018) 11843–11850.
[46] M. Yang, D. Tofan, C.H. Chen, et al., Digging the sigma-hole of organoantimony lewis acids by oxidation, Angew. Chem. Int. Ed. 57 (2018) 13868–13872.
[47] M. Yang, F.P. Gabbaï, Synthesis and properties of triarylhalostibonium cations, Inorg. Chem. 56 (2017) 8644–8650.
[48] M. Hirai, J. Cho, F.P. Gabbaï, Promoting the hydrosilylation of benzaldehyde by using a dicationic antimony-based lewis acid: Evidence for the double electrophilic activation of the carbonyl substrate, Chem. -Eur. J. 22 (2016) 6537–6541.
[49] X. Hao, T.R. Li, H. Chen, et al., Bioinspired Ether Cyclizations within a π-Basic Capsule Compared to Autocatalysis on π-Acidic Surfaces and Pnictogen-Bonding Catalysts, Chem. Eur. J. 27 (2021) 12215–12223.
[50] H.V. Humeniuk, A. Gini, X. Hao, et al., Pnictogen-Bonding Catalysis and Transport Combined: Polyether Transporters Made In Situ, JACS Au 1 (2021) 1588–1593.
[51] A. Gini, M. Paraja, B. Galmés, et al., Pnictogen-bonding catalysis: Brevetoxin-type polyether cyclizations, Chem. Sci. 11 (2020) 7086–7091.
[52] M. Paraja, A. Gini, N. Sakai, et al., Pnictogen-bonding catalysis: An interactive tool to uncover unorthodox mechanisms in polyether cascade cyclizations, Chem. -Eur. J. 26 (2020) 15471–15476.
[53] S. Benz, A.I. Poblador-Bahamonde, N. Low-Ders, et al., Catalysis with pnictogen, chalcogen, and halogen bonds, Angew. Chem. Int. Ed. 57 (2018) 5408–5412.
[54] J. Zhang, J. Wei, W.Y. Ding, et al., Asymmetric pnictogen-bonding catalysis: Transfer hydrogenation by a chiral antimony(V) cation/anion pair, J. Am. Chem. Soc. 143 (2021) 6382–6387.
[55] Q. Liu, Y. Lu, H. Sheng, et al., Visible-light-induced selective photolysis of phosphonium iodide salts for monofluoromethylations, Angew. Chem. Int. Ed. 60 (2021) 25477–25484.
[56] X. Ren, Q. Liu, Z.X. Wang, et al., Visible-light-induced direct hydrodifluoromethylation of alkenes with difluoromethyltriphenylphosphonium iodide salt, Chin. Chem. Lett. 34 (2023) 107473.
[57] F. Tan, P. Zheng, Q. Liu, et al., Charge transfer complex enabled photoreduction of Wittig phosphonium salts, Org. Chem. Front. 9 (2022) 5469–5472.
[58] C.W. Nogueira, N.V. Barbosa, J.B.T. Rocha, Toxicology and pharmacology of synthetic organoselenium compounds: An update, Arch. Toxicol. 95 (2021) 1179–1226.
[59] M. Roman, P. Jitaru, C. Barbante, Selenium biochemistry and its role for human health, Metallomics 6 (2014) 25–54.
[60] P.C. Nobre, E.L. Borges, C.M. Silva, et al., Organochalcogen compounds from glycerol: Synthesis of new antioxidants, Bioorg. Med. Chem. 22 (2014) 6242–6249.
[61] A.J. Mukherjee, S.S. Zade, H.B. Singh, et al., Organoselenium Chemistry: Role of Intramolecular Interactions, Chem. Rev. 110 (2010) 4357–4416.
[62] G. Perin, E.J. Lenardão, R.G. Jacob, et al., Synthesis of vinyl selenides, Chem. Rev. 109 (2009) 1277–1301.
[63] C.W. Nogueira, G. Zeni, J.B.T. Rocha, Organoselenium and organotellurium compounds: Toxicology and pharmacology, Chem. Rev. 104 (2004) 6255–6286.
[64] M. Birringer, S. Pilawa, L. Flohé, Trends in selenium biochemistry, Nat. Prod. Rep. 19 (2002) 693–718.
[65] G. Mugesh, W.W. Du Mont, H. Sies, Chemistry of biologically important synthetic organoselenium compounds, Chem. Rev. 101 (2001) 2125–2180.
[66] T. Wirth, Organoselenium chemistry in stereoselective reactions, Angew. Chem. Int. Ed. 39 (2000) 3740–3749.
[67] V.K. Jain, K.I. Priyadarsini, Organoselenium Compounds in Biology and Medicine: Synthesis Biological and Therapeutic Treatments, the Royal Society of Chemistry, London, 2018.
[68] J. Rafique, D.S. Rampon, J.B. Azeredo, et al., Light-mediated seleno-functionalization of organic molecules: Recent advances, Chem. Rec. 21 (2021) 2739–2761.
[69] J.A. Sehnem, F. Vargas, P. Milani, et al., Modular synthesis of chiral N-protected β-seleno amines and amides via cleavage of 2-oxazolidinones and application in palladium-catalyzed asymmetric allylic alkylation, Synthesis 2008 (2008) 1262–1268.
[70] M. Mantina, A.C. Chamberlin, R. Valero, et al., Consistent van der Waals Radii for the whole main group, J. Phys. Chem. A 113 (2009) 5806–5812.
[71] J. Contreras-García, E.R. Johnson, S. Keinan, et al., NCIPLOT: A program for plotting noncovalent interaction regions, J. Chem. Theory Comput. 7 (2011) 625–632.
[72] E.R. Johnson, S. Keinan, P. Mori-Sánchez, et al., Revealing noncovalent interactions, J. Am. Chem. Soc. 132 (2010) 6498–6506.
[73] F. Weinhold, Natural bond orbital analysis: A critical overview of relationships to alternative bonding perspectives, J. Comput. Chem. 33 (2012) 2363–2379.
[74] A.E. Reed, L.A. Curtiss, F. Weinhold, Intermolecular interactions from a natural bond orbital, donor-acceptor viewpoint, Chem. Rev. 88 (1988) 899–926.
[75] T. Lu, F. Chen, Multiwfn: A multifunctional wavefunction analyzer, J. Comput. Chem. 33 (2012) 580–592 .

Author profile

Qiang Liu (BRID: 08661.00.71527) was born in Shandong, China. He received his Ph.D. degree from RWTH-Aachen University under the supervision of Prof. Dieter Enders in 2018. After postdoctoral research in RWTH Aachen University, he joined the group of Prof. Xiang-Yu Chen in 2019 as a postdoctor. His research interest focuses on photoredox catalysis.

Xiang-Yu Chen (BRID: 07866.00.71610) was born in Shandong, China. He received his B.S. from Xiangtan University in 2009 and his Ph.D. from the Institute of Chemistry of the Chinese Academy of Sciences in 2014. After postdoctoral research at University of Vienna and RWTH Aachen University, he joined the University of Chinese Academy of Sciences as an associate professor in 2020. His research interests are asymmetric synthesis and photoredox catalysis.